International Journal of Nanoelectronics and Materials
Volume 14 (Special Issue) December 2021 [53-58]

Noise Properties of Unipolar Nanodiodes at Elevated Temperatures

Shahrir R. Kasjoo[1*], Arun K. Singh[2], Claudio Balocco[3] and Aimin Song[4]

[1]Faculty of Electronic Engineering Technology, Universiti Malaysia Perlis (UniMAP), Perlis, Malaysia
[2]Department of Electronics and Communication Engineering, Punjab Engineering College (Deemed to be University), Sector-12, Chandigarh-160012, India
[3]Department of Engineering, Durham University, DH1 3LE Durham, United Kingdom
[4]School of Electrical and Electronic Engineering, University of Manchester, M13 9PL Manchester, United Kingdom

ABSTRACT

A unipolar nanodiode known as the self-switching diode has been demonstrated as a room-temperature terahertz detector, with its noise-equivalent-power value comparable to those of the state-of-the-art Schottky diodes. Here, we study its performance at elevated temperatures and show an unusual reduction in low-frequency noise, which may be useful for practical applications. The experiments suggest that the increased thermionic emissions result in the reduced device resistance and hence the lowered noise. The observed noise behavior appears to be in good agreement with Hooge's mobility fluctuation theory.

Keywords: diode, Hooge's mobility fluctuation theory, low-frequency noise

1. INTRODUCTION

Terahertz (THz) technologies have shown many advantages in a variety of application areas including security, healthcare, telecommunication and material research. For example in healthcare, THz radiation is capable to distinguish between different human tissues based on their chemical and biological compositions [1]. It can also be used to detect many explosive and chemical weapons for security purposes. Furthermore, most clothes are transparent at THz frequencies, making concealed weapons easy to detect without the hazard of X-rays. Although some of THz-based instruments are commercially available in the market, they are relatively expensive, bulky and some of them can only operate at a very low temperature. This remains as a bottleneck in the development of compact and cost-effective THz systems.

Back in 2003, a nanodevice, known as the self-switching diode (SSD) [2], has been introduced which has shown promising properties as a microwave/terahertz detector, operating at room temperature [3]–[5]. This includes several demonstrations of THz imaging process using SSD-based detection systems [6]–[8]. Based on the simulation results in [9] and [10], SSDs also have the capability to function as THz emitters. The SSD is a unipolar two-terminal device. It consists of an asymmetric nanochannel in a semiconductor material, tailored by two insulating L-shaped trenches (see Figure 1). The asymmetry of the nanochannel results in a strong nonlinear current-voltage (*I*-*V*) behavior since the charge carrier density in the nanochannel depends on the sign of the applied voltage. This is similar to the characteristic of a typical diode but without the use of Schottky barrier structure or any doped *p*-*n* junction. This working principle allows for the SSDs to operate with a tunable threshold voltage by simply adjusting the device channel width, and a zero threshold is therefore feasible. Zero-bias THz detection is highly desired since any biasing circuitry will likely compromise the device speed and introduce low-frequency flicker noise. More details on the operating principle of SSD can be found in [2] and [9].

*shahrirrizal@unimap.edu.my

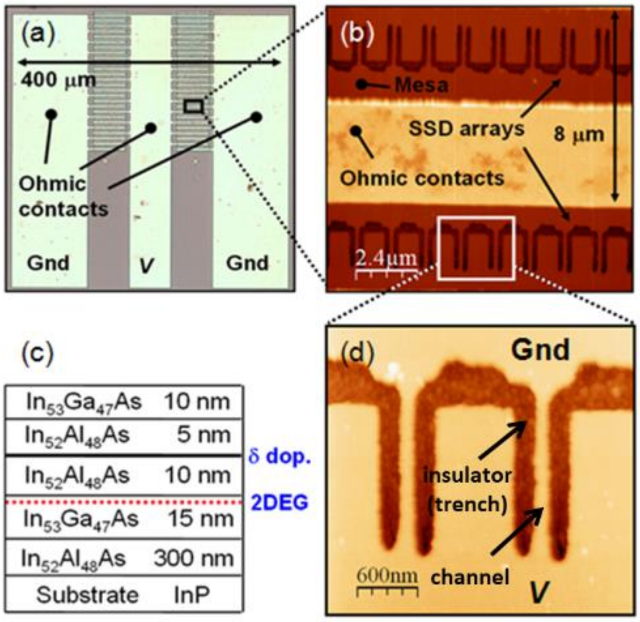

Figure 1. (a) Optical microscope image of the interdigital structure and coplanar waveguide that accommodated 2000 SSDs connected in parallel. (b) Atomic-force microscope (AFM) image of a large SSD array fabricated within the fingers of an interdigital structure. (c) Sketch of the material structure used in the fabrication. (d) AFM image showing the SSD channels were approximately 1500 nm long and 130 nm wide. The trench depth and width were 45 nm and 200 nm, respectively.

Terahertz signals detected by diode-based rectifiers are usually modulated at low frequencies, typically below 10 kHz in both direct and heterodyne detection schemes [11]. Hence, the low-frequency noise performance of the diodes is of paramount importance. Our previous work has shown comparable value of noise-equivalent-power to those reported for the state-of-the-art Schottky diodes at room temperature [12]. In this work, we study the DC and low-frequency noise characteristics of SSDs at elevated temperatures.

2. DEVICE FABRICATION

Figure 1(a) shows an interdigital structure which has been selected to house approximately 2,000 SSDs connected in parallel. This large SSD array can reduce the overall resistance of the device and hence lower the thermal noise. The array was positioned within the fingers of the interdigital structure placed in the gaps of a coplanar waveguide, as shown in Figure 1(b). The devices were fabricated on an InGaAs/InAlAs heterostructure grown onto an InP substrate (purchased from IQE Inc.). The 2-DEG layer located 25 nm below the surface as illustrated in Figure 1(c). The electron carrier density and mobility were 1.3 × 10^{12} cm^{-2} and 10,400 cm^2/Vs, respectively, as determined by Hall measurement at room temperature.

The mesa structures were firstly formed on the substrate by means of a chemical etching process with a $H_3PO_4/H_2O_2/H_2O$-based solution. The next step was to produce ohmic contacts (i.e., fingers of the interdigital structure) using thermal evaporation of a 50 nm of Au/Ge/Ni alloy followed by a 200 nm Au layer. These contacts were annealed at 390 °C. The SSD structures were then fabricated using electron-beam lithography followed by an etching process with a $Br_2/HBr/HNO_3/H_2O$-based solution. Figure 1(d) shows the atomic-force microscope image of two SSDs, connected in parallel. The SSD channels were approximately 1,500 nm long and 130 nm wide. The trench width and depth were 200 nm and 45 nm, respectively.

3. METHODS, RESULTS AND DISCUSSION

The *I-V* characteristics of the SSD array, as plotted in Figure 2, were measured in the dark at difference temperatures in a temperature-controlled stage instrument (Linkam PR600). At relatively high applied voltages, $V >> kT/q$, where k is the Boltzmann's constant, T is the absolute temperature and q is the electronic charge, the *I-V* characteristic of SSD may resemble that of a double-sided junction field-effect transistor (FET), as previously modeled by Aberg *et al.* [13]. However, when V is very small and the channel is almost completely depleted by the surface states on the sidewalls of the etched trenches, the current flowing through the channel can be approximated by an exponential curve, similar to the sub-threshold region of standard FETs:

$$I = I_0\left[\exp\left(\frac{qV}{nkT}\right)-1\right] \tag{1}$$

where I_0 and n are the fitting parameters.

Inset of Figure 2 shows the resistance of the SSD array at zero bias, R_0, as a function of temperature (estimated from Figure 2). As can be seen, the value of R_0 decreases as the temperature increases. At higher temperatures the electrons inside the SSD channels gain higher thermal energy, which enhances the thermionic emission over potential barrier. More current can therefore flow through the channels and the overall device resistance reduces. In fact, similar behavior was also reported previously by Farhi *et al* using silicon-based SSDs [14].

When a bias was applied to the SSD array, the differential resistance of the array, R can be calculated from (1) as the following,

$$R = \frac{dV}{dI} = \frac{nkT}{qI_0\left(I/I_0+1\right)} = \frac{R_0}{I/I_0+1} \tag{2}$$

Equation (2) will be used later for further analysis.

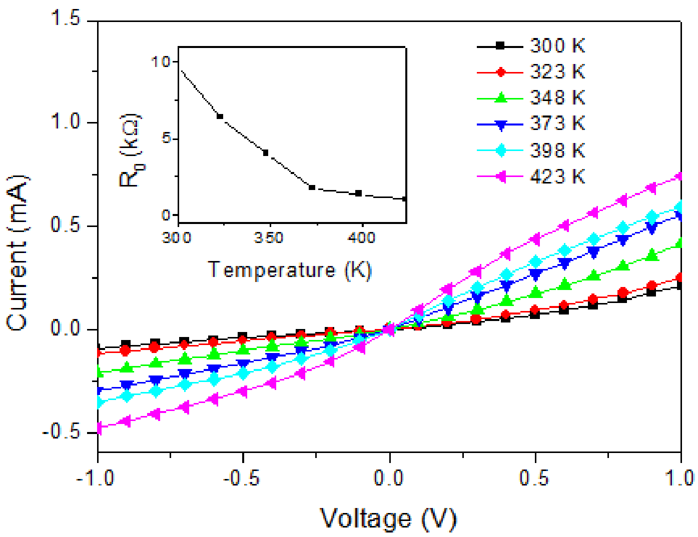

Figure 2. *I-V* characteristics of the SSD array at different *T*. The inset shows the value of R_0 of the SSD array as a function of *T*.

The low-frequency noise measurements were then conducted on the SSD array at different elevated temperatures. A two-channel cross-correlation technique [15] was employed to determine the noise power spectra from the device. The system was reported in our previous noise measurement at room temperature (details can be found in [12]). In this work, the SSD array was positioned onto a temperature-controlled-stage. The whole system was sealed with aluminum foil to screen external interference from the surroundings.

In order to avoid the 50-Hz line interference from the temperature controller, the following procedure was carried out. Firstly, the stage was heated at the set temperature and held for 10 minutes for thermal stabilization. The noise measurement was conducted immediately after the temperature controller was switched off. The device noise was measured from 10 Hz – 10 kHz, with 100 averaged spectra, which ensured that the total data-acquisition time was only approximately ten seconds. The changes in the device temperature within this period were therefore expected to be insignificant. In addition, the highest frequency of the measurement was limited by the amplifier's -3 dB bandwidth of approximately 40 kHz. This value was further reduced to 10 kHz, due to the effect of the amplifier frequency response for adopting a closed-loop circuit with non-inverting configuration [16]. Prior to the noise measurement, the system was calibrated by measuring the thermal noise of several conventional resistors in the range of 1 – 10 kΩ.

Figure 3 shows the low-frequency noise measurement of the SSD array as a function of the frequency at different temperatures. In each measurement, the DC bias V was fixed at 1.2 mV. Equation (2) can therefore be modified to $R = R_0 - (V/I_0)$. Since $R_0 >> V/I_0$, the value of R can be considered similar to R_0 (i.e., $R \sim R_0$), with an error of less than 0.5 %. Somewhat surprisingly, the $1/f$ (flicker) noise reduced as T increased. In particular, the low-frequency noise exhibited a drastic reduction, approximately by a factor of 10 at 423 K compared to that room temperature. Since the minimum detectable signal power of any THz detector (i.e., noise-equivalent power) is determined not only by the responsivity but also the device noise, the finding here may have a useful implication in SSD-based THz applications.

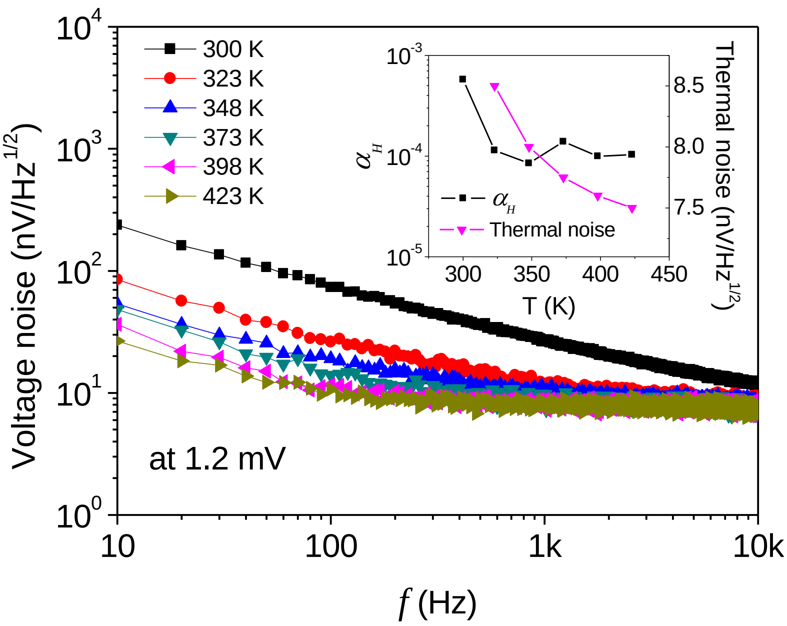

Figure 3. Voltage noise spectra of SSD array at different elevated temperatures with a constant applied voltage of 1.2 mV. The noise was reduced as T increased. The inset shows Hooge's parameter, and the thermal noise of the array as a function of T.

As can also be seen in Figure 3, the corner frequency, f_c, defined as the frequency at which the amount of $1/f$ noise equals to thermal noise, was reduced from about 10 kHz at room temperature, down to approximately 200 Hz as T approached 423 K. Moreover, at frequencies higher than f_c where the excess noise of $1/f$ can be neglected, a slightly decreased thermal noise was observed at increasing T. These estimated values of the measured thermal noise were plotted as a function of T, as shown in the inset of Figure 3. However, on average, they were approximately 30 % different to their theoretical value, $(4kTR)^{1/2}$, which was possibly due to the measurement approach used in this work. Nevertheless, both measured and theoretical values exhibit a similar decreased trend. The observed results might be useful to enhance the high-speed detection capability of the SSD array for practical applications.

To study the nature of the observed low-frequency noise, we first examined the noise spectrum in Figure 3 by fitting the experimental data into a formula based on Hooge's mobility fluctuation theory [17]. According to this theory, the noise voltage power spectra, $S_V(f)$, can be written as,

$$S_V\left(f\right)=\frac{q\mu_n V^2 R\alpha_H}{L^2 f^{\beta}} \tag{3}$$

where μ_n is the electron mobility, α_H is the Hooge's parameter, L is the length of the SSD channel, f is the frequency, and β is the fitting parameter (normally equal to 1 ± 0.1). The obtained value of β was approximately unity at all temperatures, affirming the presence of $1/f$ noise in the low frequency region. The inset of Figure 3 also shows the estimated values of α_H with respect to the elevated temperatures. As can be seen, α_H was approximately 5.75×10^{-4} at room temperature. From 323 - 423 K, the values of α_H were quite stable with an average value of around 1.08×10^{-4}.

Equation (3) explains very well the reduction of $1/f$ noise of the SSD array with increasing T. As observed earlier, the value of $R \sim R_0$ decreased as T increased. Similarly, the estimated α_H was higher at room temperature compared to that at elevated temperatures. For InGaAs/InAlAs heterostructure, it has been demonstrated that the value of μ_n in this material decreases as temperature increases [18]. Taking these factors into account, and since V and L were constant (i.e., V = 1.2 mV and L = 1,500 nm), the value of $S_V(f)$ in Equation (3) reduced with increasing temperature. This agreed very well with the results obtained in Figure 3, and has further verified that the low-frequency noise characteristic of the SSD array can be very well explained in the framework of Hooge's mobility fluctuation theory.

4. CONCLUSION

In summary, we studied the noise properties of SSDs at elevated temperatures, which might have useful implication for practical detection applications of the devices. Somewhat surprisingly, both the thermal noise and the low-frequency flicker noise were found to have improved (reduced). In particular, the flicker noise at low frequencies was reduced by almost one order of magnitude. The results suggest that the increased thermionic emissions at elevated temperatures have counteracted the decrease in carrier mobility and are responsible for the reduced resistance of the array. We show that the observed noise behavior appears to be in good agreement with Hooge's mobility fluctuation theory.

ACKNOWLEDGEMENTS

The authors would like to acknowledge all staff in the MiNE Research Group, FTKEN, UniMAP.

REFERENCES

[1] Knobloch, P., Schildknecht, C., Kleine-Ostmann, T., Koch, M., Hoffmann, S., Hofmann, M., Rehberg, E., Sperling, M., Donhuijsen, K., Hein, G., Pierz, K., Phys. Med. Biol. vol **47**, issue 21 (2002) pp. 3875-3884.

[2] Song, A. M., Missous, M., Omling, P., Peaker, A. R., Samuelson, L., Seifert, W., Appl. Phys. Lett. vol **83**, issue 9 (2003) pp. 1881-1883.

[3] Zhang, J., Brownless, J., Song, A., Nanotechnology vol **30**, (2019) pp. 364004.

[4] Balocco, C., Kasjoo, S. R., Lu, X. F., Zhang, L. Q., Alimi, Y., Winnerl, S., Song, A. M., Appl. Phys. Lett. vol **98**, issue 22 (2011) pp. 223501-223503.

[5] Kasjoo, S. R., Singh, A. K., Mat Isa, S. S., Ramli, M. M., Isa, M. M., Ahmad, N., Mohd Nor, N. I., Khalid, N., Song, A. M., Solid-State Electronics vol **118**, (2016) pp. 36-40.

[6] P. Sangare, G. Ducournau, B. Grimbert, M. Faucher, I. Iniguez-de-la-Torre, T. Gonzalez, J. Mateos, C. Gaquiere, "GaN-based Implanted Self Switching Diodes for THz Imaging," in Proc. 39th Inter. Conf. Infrared Millimeter Terahertz Waves (IRMMW-THz), Tucson, (2014).

[7] C. Balocco, Y. Pan, S. R. Kasjoo, Y. Alimi, L. Q. Zhang, A. M. Song, "THz imaging with broadband thermal sources," in Proc. 39th Inter. Conf. Infrared Millimeter Terahertz Waves (IRMMW-THz), Tucson, (2014).

[8] S. R. Kasjoo, M. B. Mohd Mokhar, N. F. Zakaria, N. J. Juhari, "A Brief Overview of Detectors Used for Terahertz Imaging Systems," in Proc. 2nd Inter. Conf. on Applied Photonics and Electronics (InCAPE), Putrajaya, (2019).

[9] Xu, K. Y., Wang, G., Song, A. M., Appl. Phys. Lett. vol **93**, issue 23 (2008), pp. 233506-233508.

[10] T. González, I. Íñiguez-de-la-Torre, D. Pardo, J. Mateos, A. M. Song, "Monte Carlo Analysis of Gunn Oscillations in Narrow and Wide Band-Gap Asymmetric Nanodiodes," in Proc. 16th Inter. Conf. on Electron Dynamics in Semiconductors, Optoelectronics and Nanostructures (EDISON 16), Montpellier, (2009).

[11] Sizov, F., Rogalski, A., Prog. Quantum Electron. vol **34**, issue 5 (2010), pp. 278-347.

[12] Balocco, C., Kasjoo, S. R., Zhang, L. Q., Alimi, Y., Song, A. M., Appl. Phys. Lett. vol **99**, issue 11 (2011) pp. 113511-113513.

[13] Åberg, M., Saijets, J., Song, A., Prunnila, M., Phys. Scr. vol **T114**, (2004) pp.123-126.

[14] Farhi, G., Saracco, E., Beerens, J., Morris, D., Charlebois, S. A., Raskin, J. -P., Solid-State Electronics vol **51**, issue 9 (2007) pp. 1245-1249.

[15] Sampietro, M., Fasoli, L., Ferrari, G., Rev. Sci. Instrum. vol **70**, issue 5 (1999) pp. 2520-2525.

[16] Adel S. Sedra, Kenneth C. Smith, "Operational Amplifiers," in Microelectronic Circuits, 4th Ed. New York: Oxford University Press, (1998) pp. 60-121.

[17] Van der Ziel, A., Proceedings of the IEEE vol **76**, issue 3, (1988).

[18] Suzuki, T., Ono, H., Taniguchi, S., Science and Technology of Advanced Materials vol **6**, issue 5 (2005) pp. 400-405.